CERN - EUROPEAN ORGANISATION FOR NUCLEAR RESEARCH

CERN/EP 79-68

29 June 1979

MUON PAIR PRODUCTION AT MASSES ABOVE 4 GeV/c^2 (DRELL-YAN CONTINUUM) BY $\pi^{\pm}$, $K^{\pm}$, $\bar{p}$ AND p OF 200 GeV/c AND BY π^- OF 280 GeV/c ON PLATINUM AND HYDROGEN TARGETS

C.E.N.,Saclay[1]-CERN[2]-Collège de France,Paris[3],
Ecole Polytechnique,Palaiseau[4]-Laboratoire de l'Accélérateur Linéaire,Orsay[5]

J. Badier[4], J. Boucrot[5], G. Burgun[1], O. Callot[5], Ph. Charpentier[1], M. Crozon[3], D. Decamp[2], P. Delpierre[3], A. Diop[3], R. Dubé[5], B. Gandois[1], R. Hagelberg[2], M. Hansroul[2], W. Kienzle[2], A. Lafontaine[1], P. Le Dû[1], J. Lefrançois[5], Th. Leray[3], G. Matthiae[2], A. Michelini[2], Ph. Miné[4], H. Nguyen Ngoc[5], O. Runolfsson[2], P. Siegrist[1], J. Timmermans[2], J. Valentin[3], R. Vanderhaghen[4], S. Weisz[2].

ABSTRACT

We have measured and analysed a total of more than 10 000 μ - pair events of the Drell-Yan type (M > 4 GeV/c^2 produced by pions, kaons, antiprotons and protons on platinum and hydrogen targets. Results are presented on scaling, A dependence, absolute comparison of $\pi^{\pm}$, $K^{\pm}$, $p^{\pm}$ induced mass spectra, P_T dependence and decay angular distributions.

EPS International Conference on High Energy Physics
Geneva, 27 June - 4 July 1979

1. INTRODUCTION

In the present paper we report our results of a comparitive study of μ-pair production in the Drell-Yan continuum ($M > 4$ GeV/c^2) by different hadrons ($\pi^{\pm}$, $K^{\pm}$, p, $\bar{p}$) incident on platinum and hydrogen targets. The data were taken at the CERN SPS (September 78 - March 79) at 200 and 280 GeV/c with the NA3 spectrometer. Results concerning the production of di-muon resonances at lower masses (ψ, ψ' and ρ, ω, ϕ) as well as the Υ (9.5 GeV) region are published in separate papers[1]. The analysis of the Drell-Yan data in terms of pion and nucleon structure functions is presented elsewhere[3].

2. EXPERIMENTAL SET-UP

The NA3 apparatus (fig. 1a) is a large acceptance spectrometer consisting of a superconducting dipole magnet and six multiwire proportional chambers. A muon filter mounted 40cm downstream of the platinum target consists of a 1.5m steel absorber having an uranium central core which covers the 30mrad forward cone. Muons are identified by a counter hodoscope mounted at the back of a 1.8m iron wall placed at the end of the experiment. More details on the experimental set-up and trigger system are given elsewhere[3]. In the π^- 280 GeV/c run, the target was a platinum cylinder 11.5cm long. In the 200 GeV/c run the target length was 6cm and a liquid hydrogen target 30cm long was placed 40cm upstream of the platinum target. For dimuon masses above 4 GeV, the distance between the two targets and between the platinum target and the beam dump were large enough to allow an unambiguous identification of the origin of the event.

Fig. 1b shows the acceptance of the apparatus for a 200 GeV/c beam, as a function of the dimuon mass M, the longitudinal momentum fraction x and transverse momentum P_t. It is calculated with the Drell-Yan model[4] using a $1 + \cos^2\theta^*$ decay angular distribution, the P_t and x dependence observed in our experiment.

Three different hadron beams were used :

(a) a negative beam of 280 GeV/c, mainly pions with an intensity of 10^7 particle/pulse.

(b) a negative beam of 200 GeV/c, with an intensity of $3 \cdot 10^7$ particle/pulse.

Kaons and antiprotons were identified by two differential Cerenkov counters CEDAR[2]. The composition of the beam was found to be : 96.3% π^-, 3.1% K^-, 0.62% $\bar{p}$.

(c) a positive beam of 200 GeV/c, with an intensity of $3 \cdot 10^7$ particle/pulse. K^+ were identified by the same two CEDAR's. In addition two threshold Cerenkov counters were used to distinguish protons from pions and kaons. The proportion of pions and kaons was enhanced by a 2 metre polyethylene absorber placed in the beam line. The composition of the beam was : 36% π^+, 4.6% K^+, 59.4% p. All Cerenkov signals were recorded by TDCs in order to measure the fraction of false particle assignments due to electronic dead-time, inefficiencies and accidental beam particles in a 4nsec coincidence window. The $\pi^\pm$, $K^\pm$, $p^\pm$ data presented here are corrected for inefficiencies and contaminations in the identification method.

3. MASS SPECTRA

Fig. 2 shows the mass spectra for the six different beam particles, measured in runs (b) and (c) on the platinum target. For π^- the actual number of events uncorrected for acceptance are plotted. For the other hadrons the numbers are normalized to the same incident particle flux. The error bars are statistical only, and there remains a systematic error in the relative normalisation of ±10% for p, $\bar{p}$, K^+, K^- due to uncertainty in the efficiency of our threshold Cerenkov and CEDAR counters. The π^+ to π^- data are normalized to within ~2%, using the equality of the ψ cross section on platinum, and our number of events in the ψ [1] signal.

The mass spectra of fig. 2 can be compared to the predictions of the Drell-Yan model[4] which assumes that the lepton pair originates, via a virtual photon, from a quark-antiquark annihilation.

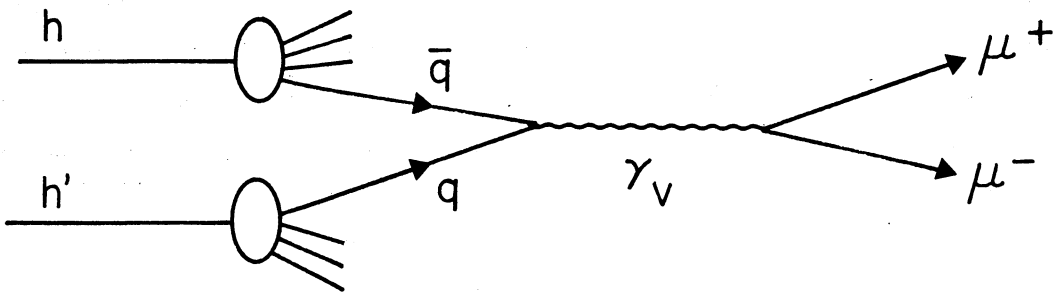

The muon pair mass M and x determine uniquely the momentum fractions x_1 and x_2 of the quark or antiquark coming from the beam and the target :

$$M^2/S = x_1 x_2, \quad x = x_1 - x_2$$

The double differential cross section can be written :

$$\frac{d^2\sigma}{dMdx} = \frac{8\pi\alpha^2}{3M^3} K \frac{1}{3} \Sigma Q_i^2 \frac{1}{x_1 + x_2} \left[f_i^h(x_1) f_{\bar{i}}^{h'}(x_2) + f_{\bar{i}}^h(x_1) f_i^{h'}(x_2) \right]$$

where $f_i^h(x)$ and $f_{\bar{i}}^h(x)$ are the structure functions of quark (antiquark) having flovor i in hadron h(h'). The factor 1/3 is due to the color hypothesis, and Q_i is the charge of quark i. The valence structure functions are normalized to give the correct number of quarks. K is a scale factor, related either to our experimental normalisation error or a physical multiplicative correction factor (e.g. QCD effects). The high statistics π^- and π^+ data are used to determine the pion and proton structure functions[3]. This analysis gave the following result :

π^- valence	$V(x) = 0.55x^{0.4}(1 - x)^{0.9}$
π sea	$S^{\pi}(x) = 0.09(1 - x)^{4.4}$
p valence up	$u(x) = 10.5x^{1.02}(1 - x)^{4.0}$
p valence down	$d(x) = 6.3x^{1.02}(1 - x)^{5.0}$
p sea	$S^{N}(x) = 0.35(1 - x)^{6.0}$
	$K = 1.4$

We assume the same value of K for the six reactions $\pi^{\pm}$, $K^{\pm}$, $p^{\pm}N \rightarrow \mu^+\mu^-X$.

We also assume that the pion and the proton seas are SU3 symmetric. We suppose exact SU3 invariance to determine the kaon structure functions from the pion ones. The curves of fig. 2 represent the result of the predictions of the model, corrected by our experimental acceptance.

One observes that the K^+ induced mass spectrum is below the K^- spectrum by a factor of 4.5; this could be explained by the fact that the K^- meson contains a valence antiquark $\bar{u}$ which annihilates with the u valence quark of the proton, whereas in the case of the K^+ a $\bar{s}$ valence can only annihilate with the strange sea of the proton. In the hypothesis of SU3 invariance, the K^- induced mass spectrum is expected to be equal to π^-. This prediction is compatible with our data, within the present error.

For incident nucleons (p, $\bar{p}$, fig. 2), again using the same scale factor K as for the mesons and the nucleon structure functions derived above, the predictions do not fit the data. For the proton, the curve is a factor ~3 higher than the data points. This discrepancy could be due to a too high value of the nucleon sea, determined from pion data[3]. We have also computed the expected mass spectra using the CDHS structure functions[6] (at $Q^2 = -20$ GeV^2) as input, both for the target nucleon and the projectile in the case of incident p and $\bar{p}$ (fig. 2c). We used a scale factor K = 2.5 as derived from the CDHS analysis of our π data [3]; the result are compatibile with the data and are shown as dashed lines in fig.2.

4. CHARGE ASYMMETRY ($\sigma(\pi^+)/\sigma(\pi^-)$ ratio)

A more detailed comparison of the π^+ and π^- spectra is represented by their ratio as shown in fig. 3. This ratio is equal to 1.01 ± 0.02 at the ψ mass and falls towards 0.35 at high mass, except in the upsilon region. A value of $\sigma(\pi^+)/\sigma(\pi^-) = 1/4$ is expected in the Drell-Yan model for an isoscalar target at large x_1 and x_2 (pion valence antiquark and proton quark dominate over the sea). On a platinum target (40% protons and 60% neutrons), the value depends on the u/d ratio at $x_2 \to 1$: $\sigma(\pi^+)/\sigma(\pi^-) = 0.286$ for $u/d \to 2$, 0.327 for $u/d \to 5$[5] and = 0.375 for $u/d \to \infty$[6]. Data points are also presented for the hydrogen target where the expected $\sigma(\pi^+)/\sigma(\pi^-)$ ratios are 0.125, 0.05 and 0. respectively. With the present data we cannot distinguish between the different predictions.

5. THE A-DEPENDENCE

A comparison between the hydrogen and platinum data has been made in order to obtain the A-dependence of our D.Y. cross section parametrized as A^α. A correction for the I-spin asymmetry of the Pt nucleus has been obtained from the $\pi^-\pi^+$ difference which also eliminates sea quark effects. We measure the experimental ratio of $\pi^- - \pi^+$ cross sections, multiplied by A, to be :

$$A \frac{\sigma_H}{\sigma_{Pt}} = 1.51 \pm 0.28$$

If u and d are the up and down quarks in the proton, the expected

ratio is :

$$A \frac{\sigma_H}{\sigma_{Pt}} = A^{1-\alpha} \frac{<4u - d>}{<u + 2d>}$$

since u = 2d, we have :

$$\frac{< 4u - d >}{< u + 2d >} = 1.75$$

If we now use the Field-Feynman hypothesis, $d = 1.125u/2(1 - x_2)$, this number becomes 1.80, and we thus obtain (*) :

$$A^{1-\alpha} = 0.84 \pm 0.16$$

Thus our α value for the Drell-Yan process is

$$\alpha = 1.03 \pm 0.03$$

This value supports the hypothesis of incoherent parton interactions. Previous experiments measured this parameter and found $\alpha = 1.02$ for proton-nucleus interaction[11] and $\alpha = 1.12 \pm 0.05$ for pion-nucleus interaction[10].

6. SCALING

The scaling hypothesis states that $M^3 d\sigma/dM$ is a function of M^2/S only. The Drell-Yan model satisfies this property, if the structure functions do not depend on M^2 (the $\log Q^2$ dependence observed in deep inelastic neutrino scattering[7], and predicted by QCD, produces only a very small effect in the $Q^2 = -M^2$ range we explore by comparing runs (a) and (b)). A lack of scaling in $\pi^- N \to \mu^+ \mu^- X$ has been proposed[8] in order to reconcile data taken from different experiments. Most of the difference between the data of K.J. Anderson et al.[10] at 225 GeV/c and our data is due to their choice of the A^α dependence : $\alpha = 1.12$. With a choice of $\alpha = 1$, their $d\sigma/dM$ per nucleon would be higher by a factor 1.8. We can compare our data at 200 and 280 GeV/c in the same apparatus and on the same target. Fig. 4 shows a good compatibility between the two energies, except in the upsilon region

---

(*) Re-interactions in the 6cm platinum target was account for (10 ± 5)% of the cross section at the ψ mass; we estimate this effect to be ~5% for the Drell-Yan data. We do not correct for this effect.

as expected. Thus the scaling property is well satisfied in our data, within the normalization error of ±15%.

Another variable was investigated for scaling : in fig. 5 we give the mean value of $X = 2P_L^*/\sqrt{s}$, as a function of $M/\sqrt{s}$, for π^- at 200 GeV/c and 280 GeV/c. A regular increase of $< x >$ with $M/\sqrt{s}$ is observed. The two distributions are comparable.

7. TRANSVERSE MOMENTUM

In table 1 and 2 the mean transverse momentum and the mean transverse momentum squared are summarized as a function of the dimuon mass, for all incident particles in run (a), (b) and (c) on the platinum target. Fig. 6 shows $< P_t >$ for π^+, π^- and p with points from other experiments[9,10] for comparison. A good compatibility is found for π^- and p : the pion $< P_t >$ reaches about 1.2 GeV/c and the proton $< P_t >$ about 1 GeV/c. π^+ and π^- data show a similar behaviour.

We have also determined $< P_t >$ and $< P_t^2 >$ on the hydrogen target for runs (b) and (c). The data are presented in table 3. No large deviation is observed relative to the platinum data.

8. ANGULAR DISTRIBUTION

Fig. 7 shows, for π^- run (b), the distribution of the cosine of the Gottfried-Jackson dimuon decay angle θ^*. The data are restricted to $P_T < 1$ GeV/c to avoid a smearing of the axis, and to $4 < M < 6$ GeV/c^2. A fit of the formular $1 + \lambda\cos^2\theta^*$ gives $\lambda = 0.80 \pm 0.17$ with a χ^2 of 12.1 for 7 degrees of freedom. A χ^2 of 13.5 is obtained when the value of λ is fixed at 1. The Collins-Soper decay angle[12] gives the fitted value : $\lambda = 0.85 \pm 0.17$ with a χ^2 of 10.5. In the Drell-Yan model, these angle definitions are equivalent, since the transverse momentum is not taken into account. Thus the prediction $\lambda = 1$ is compatible withour data.

9. CONCLUSION

We have measured with a large statistics the production of dimuon on platinum and hydrogen by $\pi^\pm$, $K^\pm$ and $p^\pm$ beams, at masses higher than 4 GeV/c^2.

Using the structure functions determined in this experiment with the $\pi^{\pm}$ data, we can roughly reproduce the shape of the mass spectra for all incident particles. However a constant scale factor K = 1.4, derived from the $\pi^{\pm}$ data, seems to be inadequate to reproduce the p (and possibly $\bar{p}$) mass spectrum in absolute value.

The dimuon decay angle is fitted with a $1 + \lambda\cos^2\theta^*$ distribution, with $\lambda = 0.80 \pm 0.16$ (Gottfried-Jackson) or $\lambda = 0.85 \pm 0.17$ (Collins-Soper).

Comparing platinum and hydrogen data, we measure a value of the α parameter for the A-dependence : $\alpha = 1.02 \pm 0.03$. $M^3 d\sigma/dM$ scaling is observed for the π^- events at 200 and 280 GeV/c. We also find that $< X >$ scales in $M/\sqrt{s}$.

Mass dependence of $< P_t >$ and $< P_t^2 >$ are given for all incident particles. They are higher in π^+ and π^- ($< P_t > = 1.12$ GeV/c) than for proton ($< P_t > = 1.01$ GeV'c).

REFERENCES

(1) J. Badier et al., "Dimuon resonance production from 200 and 280 GeV/c tagged hadron beam", International Conference on High Energy Physics, Geneva 1979.

(2) C. Bovet et al., CERN-SPS/EPP/77.19.

(3) J. Badier et al., "Experimental determination of the pion and nucleon structure functions by measuring high-mass muon pairs produced by pions of 200 and 280 GeV/c", International Conference on High Energy Physics, Geneva 1979.

(4) S.D. Drell and T.M. Yan, Phys. Rev. Letters 25 (1970) 316.

(5) G.R. Farrar and D.R. Jackson, Phys. Rev. Letters 35 (1975) 1416.

(6) R.D. Field and R.P. Feynman, Phys. Rev. D15 (1977) 2590.

(7) J.G.H. de Groot et al., Phys. Letters 82B (1979) 456.

(8) G.E. Hogan et al., Phys. Rev. Letters 42 (1979) 948.

(9) J.K. Yoh et al., Phys. Rev. Letters 41 (1978) 684.

(10) K.J. Anderson et al., Phys. Rev. Letters 42 (1979) 944.

(11) D.M. Kaplan et al., Phys. Rev. Letters 40 (1978) 435.
L.M. Lederman, in proceedings of the nineteenth International Conference of High Energy Physics, Tokyo, Japan 1978.

(12) J.C. Collins and D.E. Soper, Phys. Rev D16 (1977) 2219.

Table 1

$< P_t >$ versus M

	200 GeV/c						280 GeV/c
	π^-	K^-	$\bar{p}$	π^+	K^+	p	π^-
Number of events	5916	119	54	2195	215	1304	5700
4 < M < 5	1.10 ± 0.02	1.09 ± 0.13	1.22 ± 0.24	1.09 ± 0.03	1.08 ± 0.10	1.02 ± 0.04	1.18 ± 0.02
5 < M < 6	1.12 ± 0.03	1.12 ± 0.31	1.05 ± 0.27	1.11 ± 0.06	1.20 ± 0.25	0.96 ± 0.07	1.20 ± 0.04
6 < M < 7	1.17 ± 0.05			1.02 ± 0.08	0.84 ± 0.28	1.03 ± 0.17	1.31 ± 0.06
7 < M < 8	1.25 ± 0.08			1.16 ± 0.14		0.96 ± 0.26	1.33 ± 0.09
8 < M < 9	1.23 ± 0.12			1.42 ± 0.25			1.28 ± 0.11
9 < M <10	1.22 ± 0.16			1.15 ± 0.20			1.38 ± 0.15
10 < M <11	1.33 ± 0.15			1.21 ± 0.36			1.25 ± 0.20

Table 2

$< P_t^2 >$ versus M

	200 GeV/c						280 GeV/c
	π^-	K^-	$\bar{p}$	π^+	K^+	p	π^-
4 < M < 5	1.62 ± 0.04	1.53 ± 0.23	1.81 ± 0.42	1.58 ± 0.06	1.69 ± 0.23	1.40 ± 0.07	1.90 ± 0.06
5 < M < 6	1.70 ± 0.07	1.73 ± 0.61	1.37 ± 0.44	1.66 ± 0.12	1.91 ± 0.55	1.27 ± 0.12	1.98 ± 0.09
6 < M < 7	1.82 ± 0.11			1.35 ± 0.15	0.97 ± 0.40	1.36 ± 0.12	2.29 ± 0.14
7 < M < 8	2.13 ± 0.20			1.85 ± 0.32		1.15 ± 0.43	2.38 ± 0.22
8 < M < 9	2.00 ± 0.25			2.48 ± 0.55			2.16 ± 0.24
9 < M <10	2.02 ± 0.32			1.70 ± 0.37			2.55 ± 0.37
10 < M <11	2.36 ± 0.60			2.12 ± 0.89			2.28 ± 0.58

Table 3

	π^-	π^+	p
Number of events	138	47	24
$< P_T >$	1.01 ± 0.10	1.17 ± 0.20	0.95 ± 0.22
$< P_T^2 >$	1.38 ± 0.17	1.85 ± 0.37	1.11 ± 0.30

Figure captions

Fig. 1 (a) General layout of the experiment.

(b) Acceptance of the apparatus, as a function of $x = 2P_L^*/\sqrt{s}$, of the transverse momentum P_t and of the dimuon mass M.

Fig. 2 Dimuon mass spectra induced by $\pi^{\pm}$(a), $K^{\pm}$(b), $p^{\pm}$(c), not corrected for acceptance. Data are normalized to the same number of beam particles. Curves are predictions of the Drell-Yan model (see text). Dashed lines : CDHS fits used as input[6].

Fig. 3 Ratio of π^+/π^- cross sections, as a function of M, for the platinum and hydrogen targets. The two curves show the predicted ratios $\sigma(\pi^+)/\sigma(\pi^-)$ for the platinum and hydrogen data, respectively, using the structure functions derived from our π data.

Fig. 4 Plot of $M^3 d\sigma/dM$, as a function of $\sqrt{\tau} = M/\sqrt{s}$ for π^- at 200 and 280 GeV/c^2.

Fig. 5 Mean x, function of $\sqrt{\tau} = M/\sqrt{s}$ for π^- at 200 and 280 GeV/c.

Fig. 6 Mean transverse momentum, as a function of M, for p, $\pi^{\pm}$ (200 GeV/c) and π^- (280 GeV/c) beams.

Fig. 7 Distribution of $\cos\theta^*$ (Gottfried-Jackson angle) for π^- 200 GeV/c, with the cuts $4 < M < 6$ GeV/c^2, $P_t < 1$ GeV/c^2.

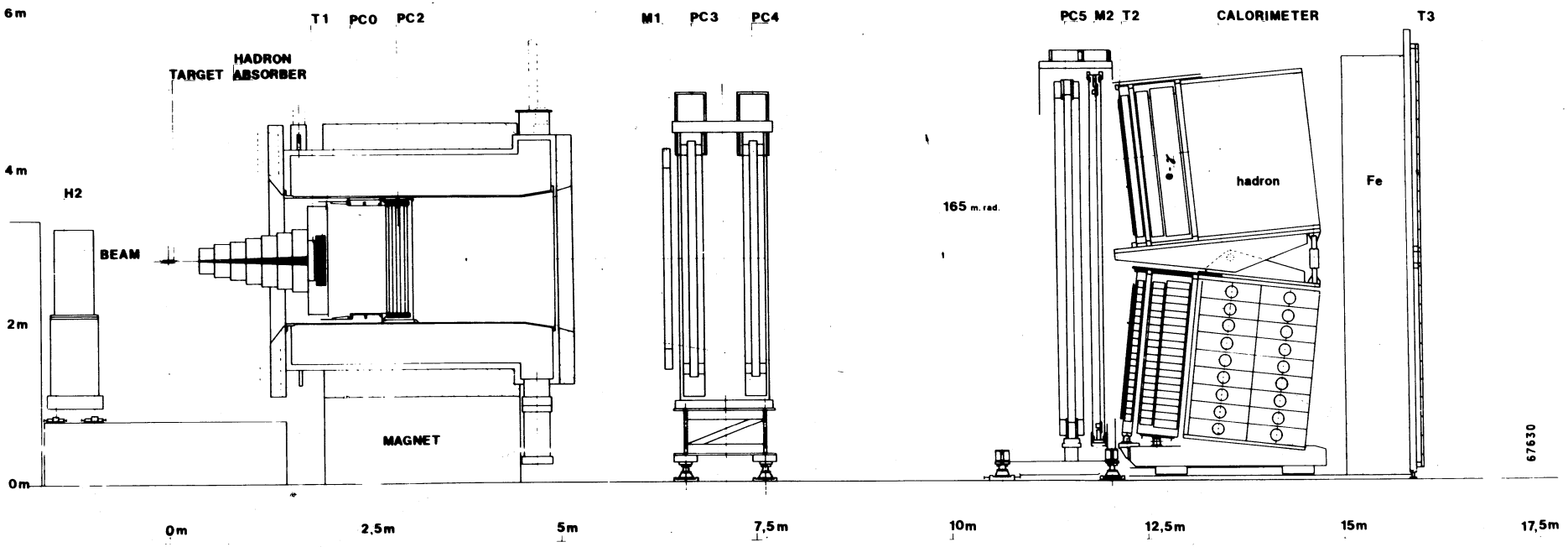

FIG. 1a Experimental layout / side view

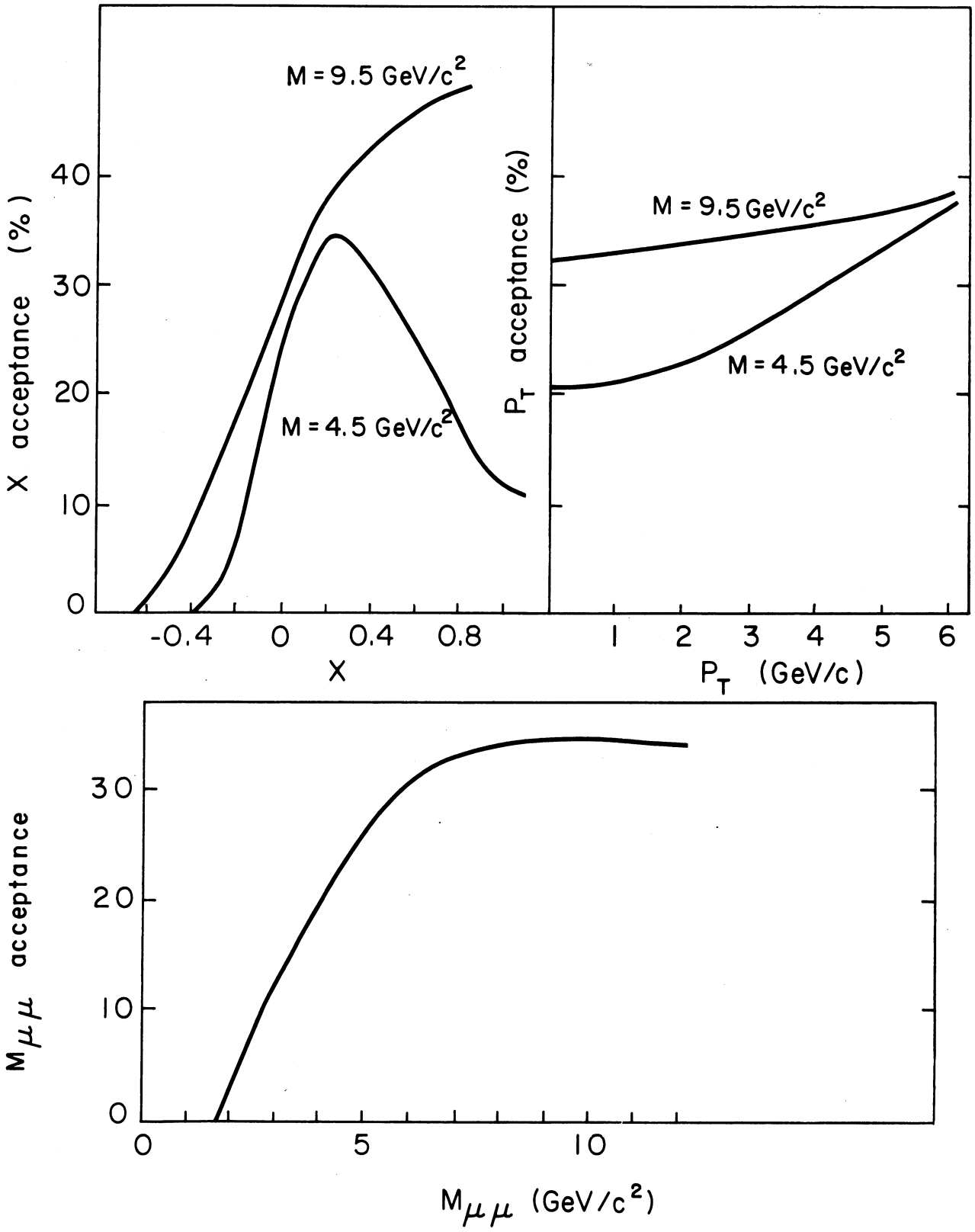

FIG. 1b : Acceptance 200 GeV/c

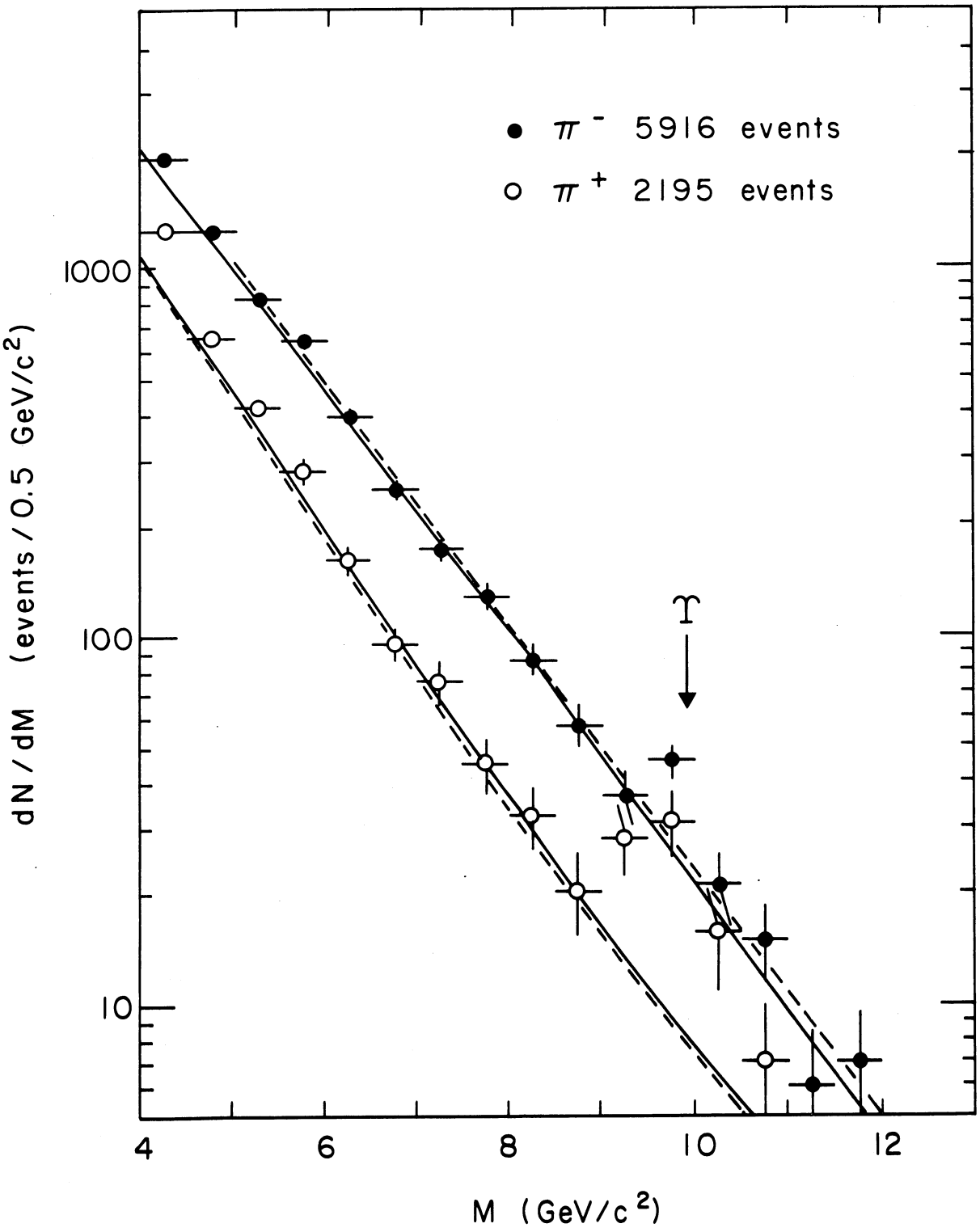
● π⁻ 5916 events
○ π⁺ 2195 events
Υ
1000
100
10
4
6
8
10
12
dN / dM (events / 0.5 GeV/c²)
M (GeV/c²)

FIG. 2 a

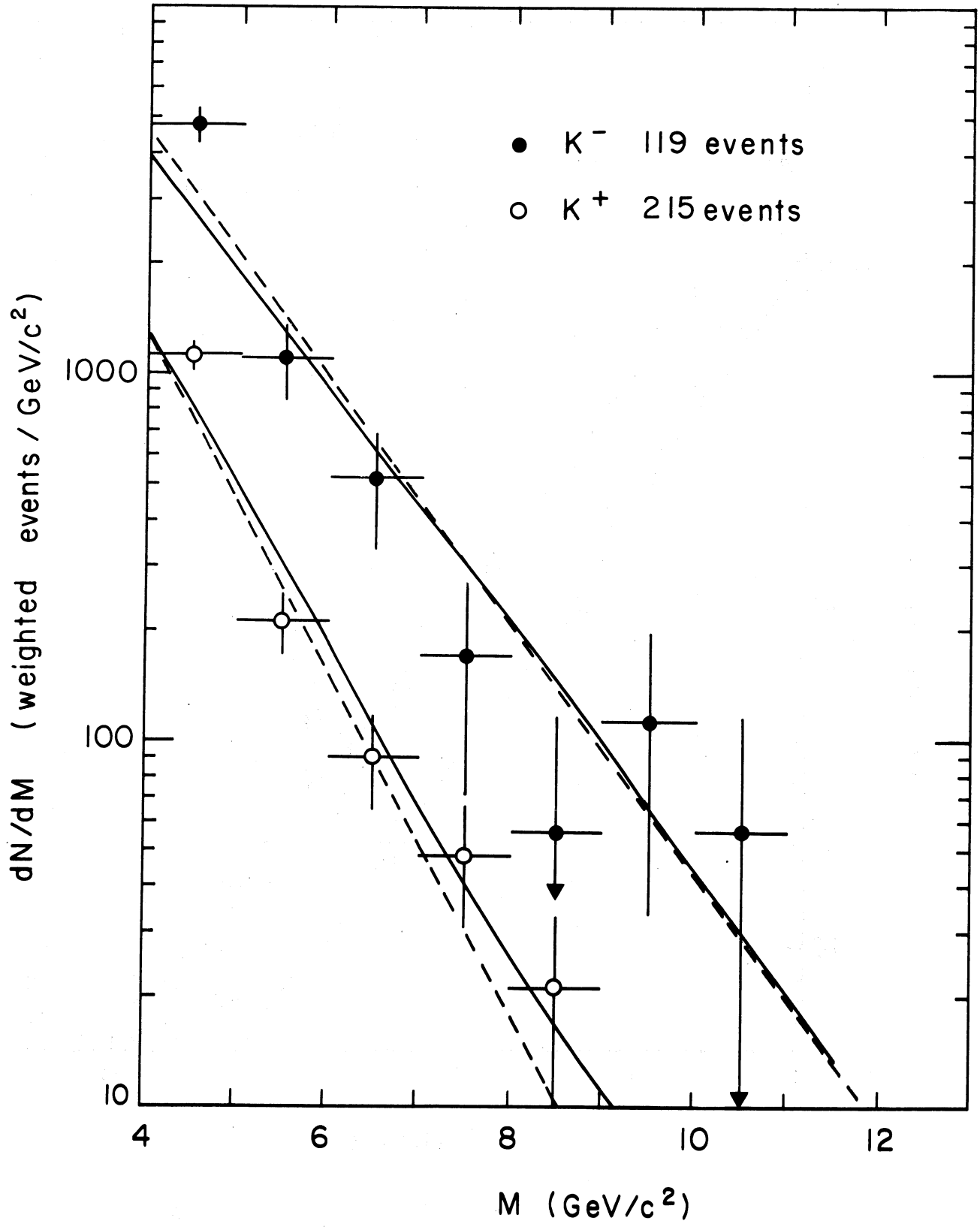
K⁻ 119 events
K⁺ 215 events
dN/dM (weighted events / GeV/c²)
1000
100
10
4
6
8
10
12
M (GeV/c²)

FIG. 2 b

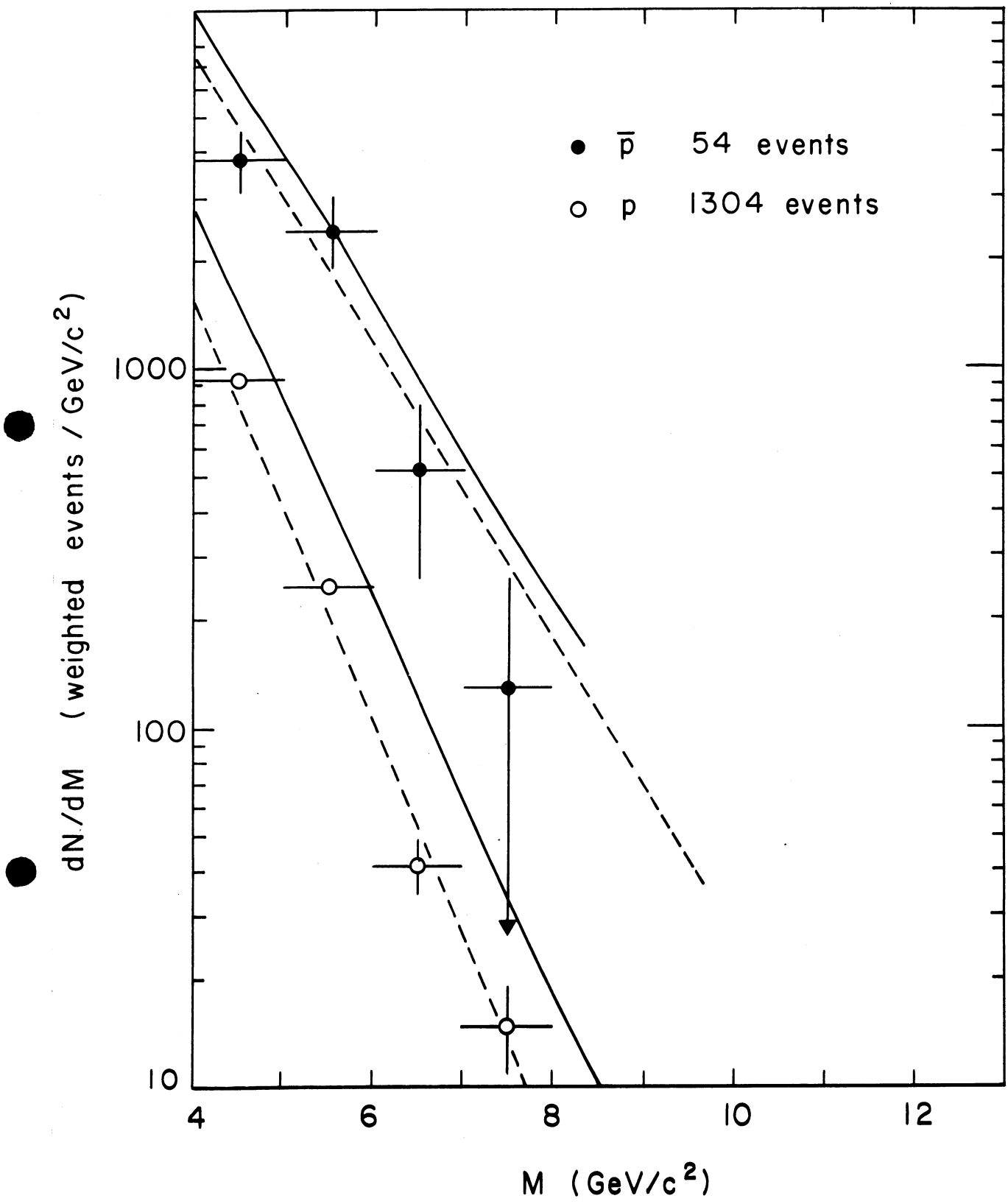
● $\bar{p}$ 54 events
○ p 1304 events
dN/dM (weighted events / GeV/c²)
1000
100
10
4
6
8
10
12
M (GeV/c²)

FIG. 2c

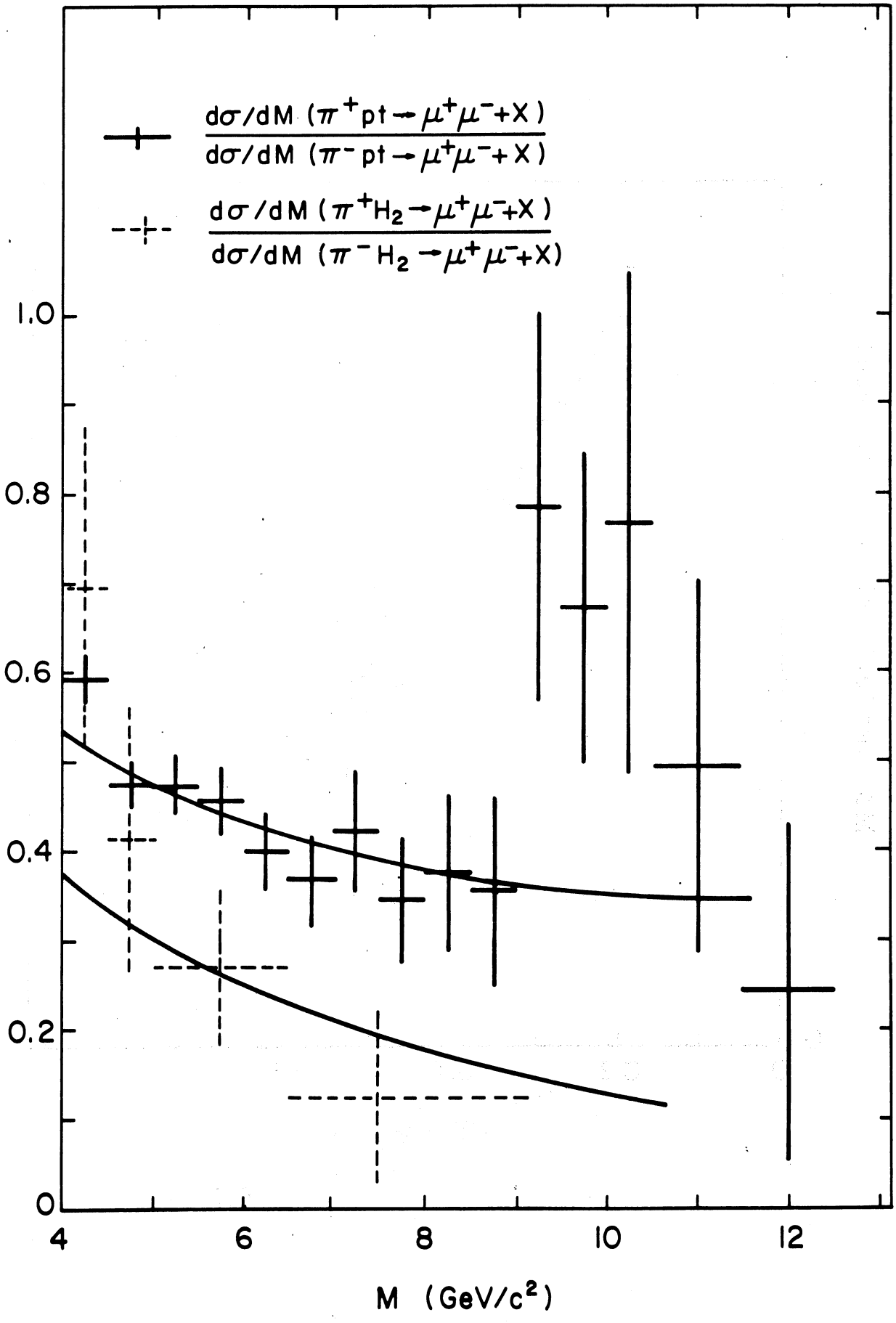
$\frac{d\sigma/dM\,(\pi^+ pt \to \mu^+\mu^- + X)}{d\sigma/dM\,(\pi^- pt \to \mu^+\mu^- + X)}$
$\frac{d\sigma/dM\,(\pi^+ H_2 \to \mu^+\mu^- + X)}{d\sigma/dM\,(\pi^- H_2 \to \mu^+\mu^- + X)}$
1.0
0.8
0.6
0.4
0.2
0
4
6
8
10
12
M (GeV/c²)

FIG. 3

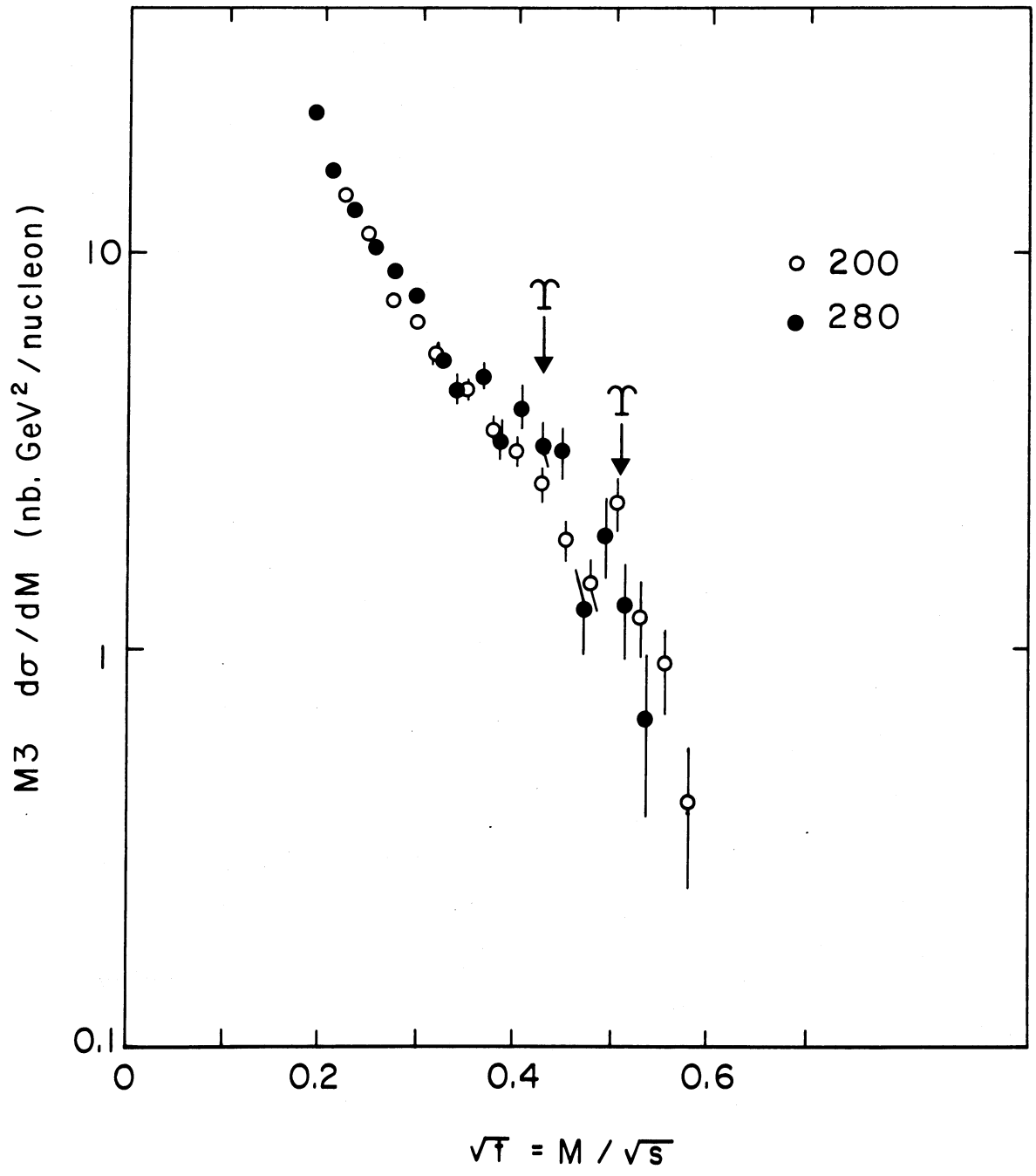

FIG. 4

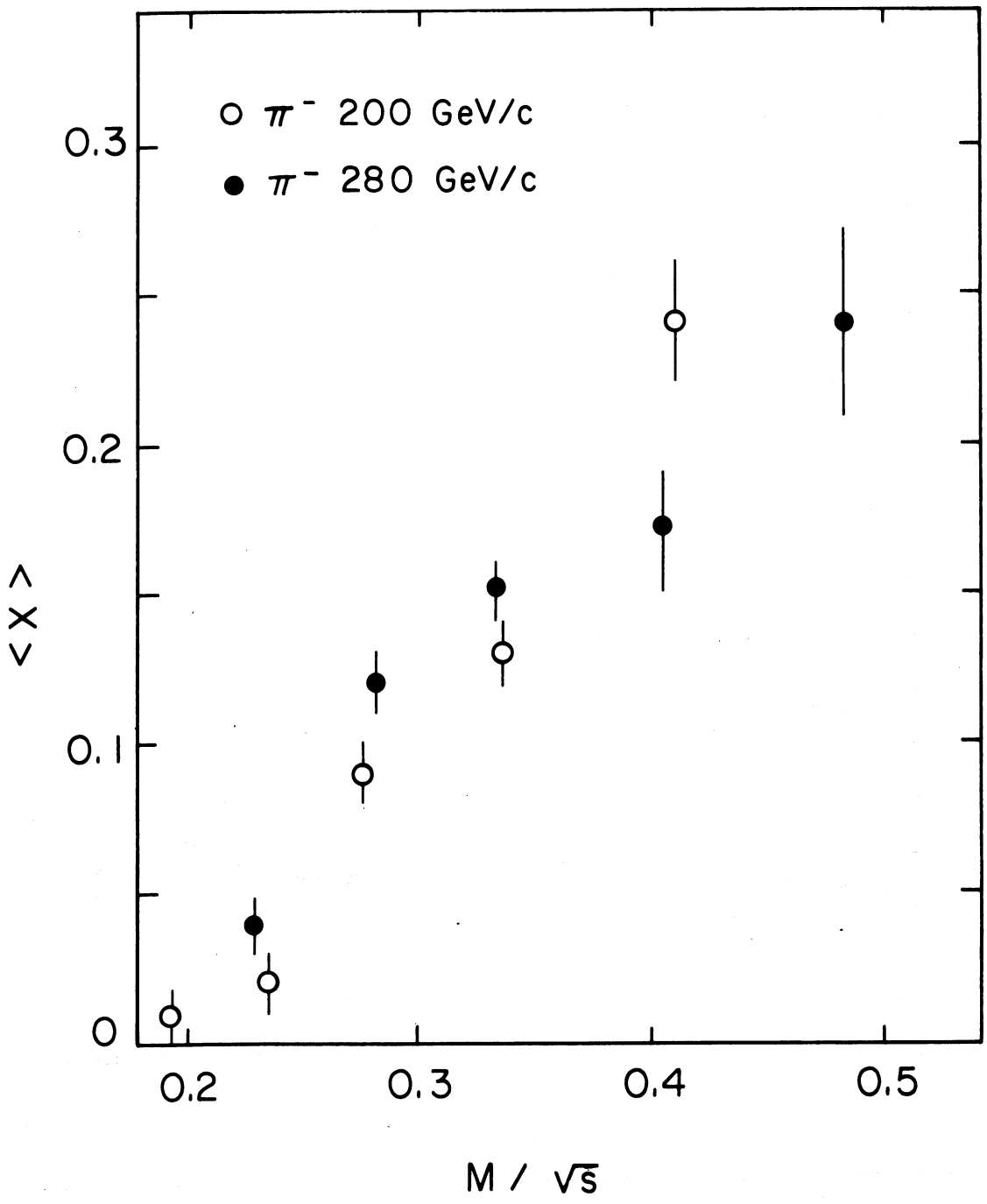

FIG. 5

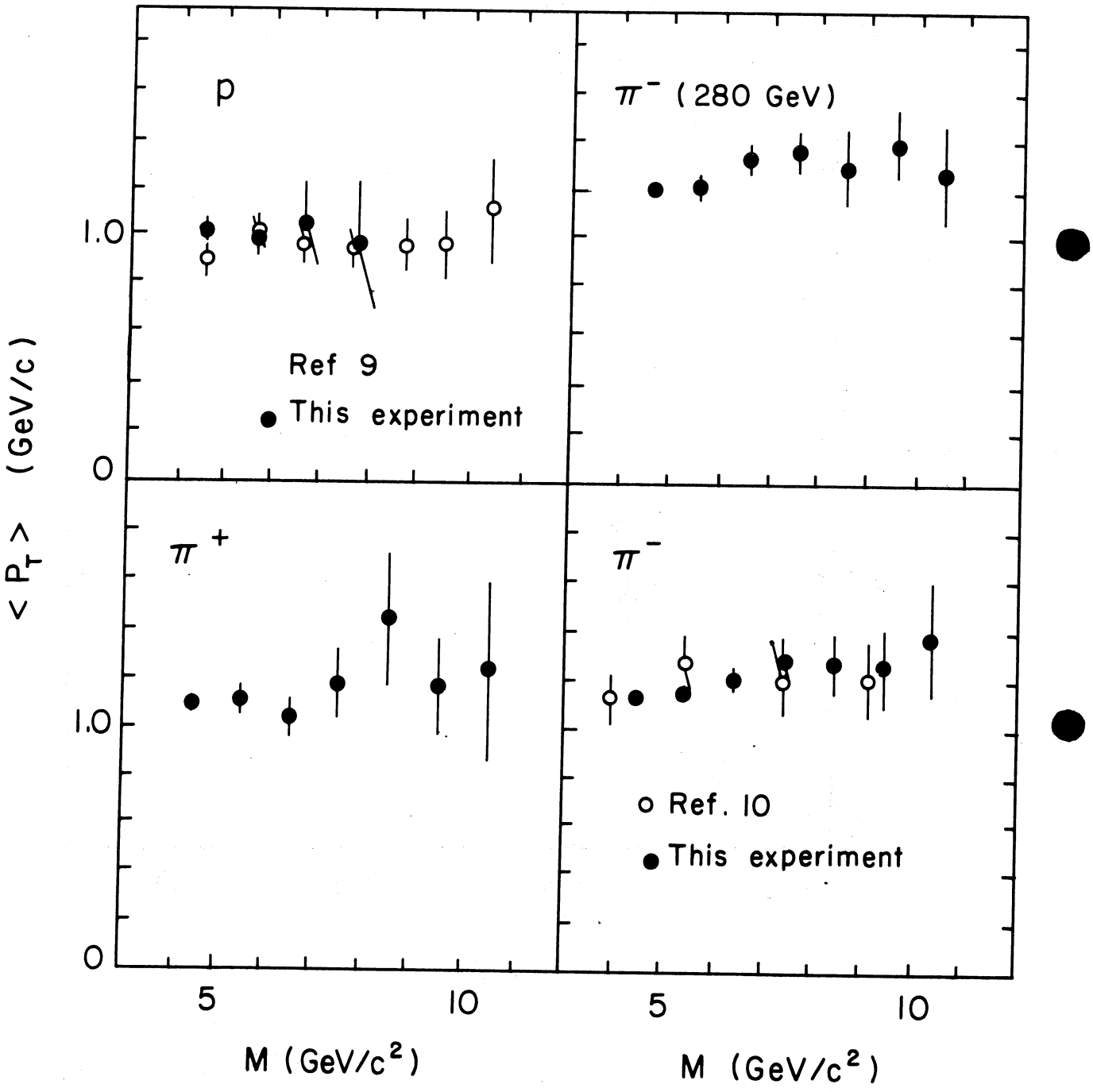
p
π⁻ (280 GeV)
π⁺
π⁻
Ref 9
This experiment
Ref. 10
This experiment
1.0
0
5
10
M (GeV/c²)
< P_T > (GeV/c)

FIG. 6

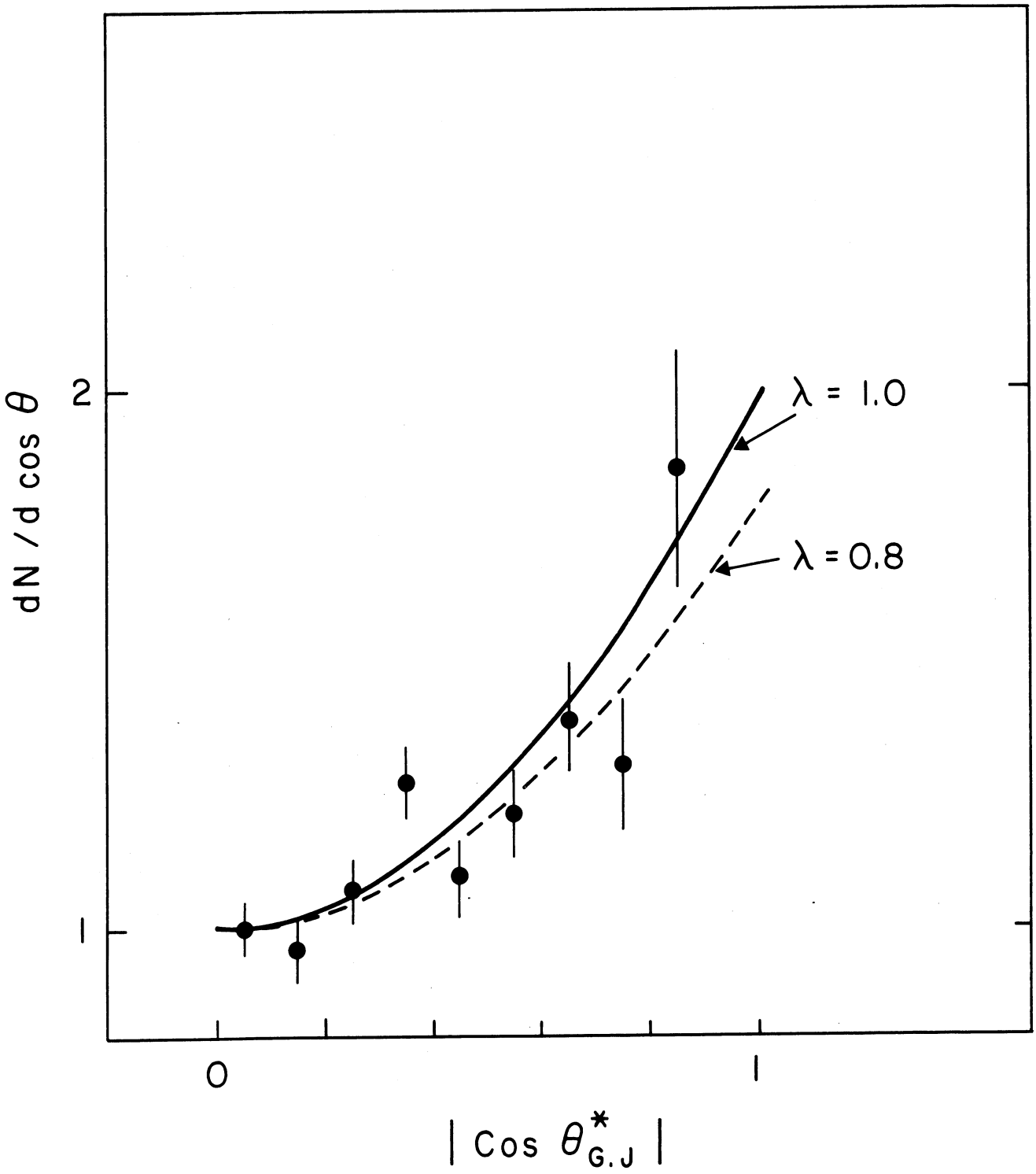

FIG. 7